Virus Therapy of Glioblastomas

V.L. de Rioja[1*], N. Isern[1], J. Fort[1] & J.M. Cobo[1]

[1] Complex Systems Laboratory, Universitat de Girona, Girona (Spain)

* victor.lopezd@udg.edu

Introduction

Clinical research has shown that the treatment of glioblastomas (GBM) could benefit from oncolytic virus therapy. Vesicular Stomatitis Virus (VSV) is one of the best candidates due to its strong oncolytic properties.

Biophysical models have been developed to describe virus treatment of tumors, though they are usually not compared quantitatively to experimental results.

Our research focuses on the development of a mathematical model for the VSV-GBM system which can explain satisfactorily the virus-tumor dynamics and reproduce the experimental in vitro propagation speeds.

Reaction-Diffusion Model

We have developed the models below in order to explain a particular in vitro VSV-GBM experiment: a virus injected into the center of the tumor spreads through a two-dimensional geometry.

Viruses diffuse through the medium before infecting tumor cells. When infected cells die, a new generation of viruses is created and the process begins anew. So, essentially the process is described by the reactions

$$V + T \xrightarrow{k_1} I \xrightarrow{k_2} Y \cdot V \qquad (1)$$

We present three increasingly realistic models using partial differential equations to describe the spatiotemporal dynamics of the virus-tumor system.

Model 1: Based on the studies of Wodarz [1] and Nowak and May [2], their equations are modified to fit our more complex VSV-GBM problem: no homogeneous system $\Rightarrow \frac{\partial^2[V](r,t)}{\partial r^2} \neq 0$; no free virus in steady-state $\Rightarrow \frac{\partial[V](r,t)}{\partial t} \neq 0$; virus population number is reduced due to adsorption. (Blue terms in Eqs. (2)-(5)).

Model 2: Infected tumoral cells do not die instantly; there is a time delay τ before the cell dies and releases the new progeny of viruses. This fact is included by adding the red terms into Eqs. (4) and (5).

Model 3: Fickian's diffusion (used in models 1 and 2) does not consider the time interval during which a virus does not move in space. Second-order temporal derivatives are included to incorporate the diffusive time-delay effect (green terms in Eqs. (2) and (6)). Higher orders are excluded because they yield similar results.

Eqs. (2)-(6) describe the 3 models, with each term color coded in agreement with the model that incorporates it [3].

$$\frac{\partial[V](r,t)}{\partial t} + \frac{\tau}{2}\frac{\partial^2[V](r,t)}{\partial t^2} = D_{VSV}\frac{\partial^2[V](r,t)}{\partial r^2} + F(r,t) + \frac{\tau}{2}\left.\frac{\partial F(r,t)}{\partial t}\right|_g, \qquad (2)$$

$$\frac{\partial[T](r,t)}{\partial t} = D_{GBM}\frac{\partial^2[T](r,t)}{\partial r^2} - k_1[V](r,t)[T](r,t) + a[T](r,t)\left\{1 - \frac{[I](r,t)+[T](r,t)}{k}\right\}, \qquad (3)$$

$$\frac{\partial[I](r,t)}{\partial t} = k_1[V](r,t)[T](r,t) - k_2[I](r,t-\tau), \qquad (4)$$

where

$$F(r,t) = -k_1[V](r,t)[T](r,t) + k_2 Y[I](r,t-\tau) - k_3[V](r,t), \qquad (5)$$

$$\left.\frac{\partial F(r,t)}{\partial t}\right|_g = -k_1 F(r,t)[T](r,t) - k_1[V](r,t)\frac{\partial[T](r,t)}{\partial t} + k_2 Y\frac{\partial[I](r,t-\tau)}{\partial t} - k_3 F(r,t) \qquad (6)$$

Results

Tumor front

For all three models, tumor expansion takes place independently of the infection front and according to a single and simple analytical solution [3]:

$$c_{GBM} = 2\sqrt{D_{GBM}\cdot a}. \qquad (7)$$

Using the parameters in Table 1, we obtain the range: $7.90\cdot10^{-5} < c_{GBM} < 4.33\cdot10^{-4}\ cm/h$ [3], which is consistent with experimental results [4].

Infection front

The virus front speed is calculated numerically from Eqs. (2)-(6) for each model by assuming solutions of the type $[V] = \epsilon\cdot e^{-\lambda(r-c\cdot t)}$. As τ has not been accurately measured, Figure 1 shows the infection front speed as a function of the delay time $c(\tau)$.

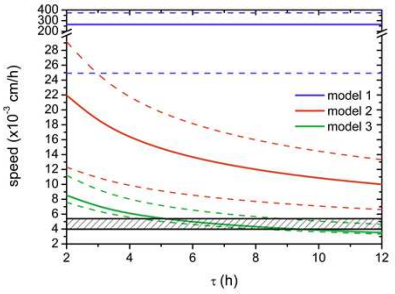

Fig. 1 VSV front propagation speed as a function of the delay time τ for model 1, model 2 and model 3. The hatched area shows the experimental in vitro VSV front speed [9]. Solid curves are calculated from typical or average parameter values; dashed curves correspond to the upper and lower bounds of the parameters in Table 1. (Figure adapted from Fig. 2 in Ref. [3]).

Model 1: The speeds are much faster than the observed. Results are constant because the model does not depend on τ.

Model 2: Much better results are achieved (yet, not enough to explain the experimental data) only by considering the delay time on the terms of death of infected cells.

Model 3: By incorporating the second-order terms into Eq. (2) the resulting front speed is in agreement with the experimental data if $5.0 < \tau < 9.3\ h$.

Numerical simulations

We also solved model 3, Eqs. (2)-(6), by numerical integration, obtaining results consistent with those from Fig. 1 (relative errors are lower than 2.5%). Numerical integration also allows the visualization of the moving fronts of viruses and infected cells. In Fig. 2 we see that, at the edge of the infection front, the number of infected cells grows rapidly, and that then there is a plateau as a result of the time delay τ. After this interval, the number of infected cells starts to decay producing a rise in the virus population.

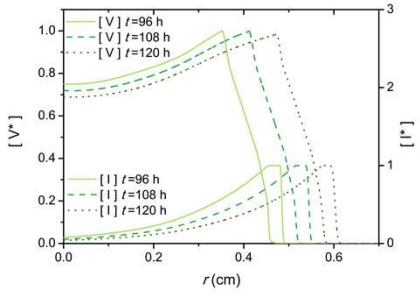

Fig. 2 Radial profiles for viruses and infected cells $[V^*] = \frac{[V]}{[V]_{max}}$ and $[I^*] = \frac{[I]}{[I]_{max}}$ at three different times for model 3. Zooming in would show that $[V^*]$ and $[I^*]$ share the same edge of the front. (Adapted from Fig. 3 in Ref. [3]).

Parameter values

All parameters used in the models are estimated from independent experiments for VSV and GBM and, when possible, from in vitro experiments on VSV applied to GBM [4-9].

Table 1 Experimental parameter values and references to the sources

Parameter [unit]	Value	Ref.
$D_{VSV}\ [cm^2/h]$	$\mathbf{8.37\cdot10^{-5}}$ and $1.44\cdot10^{-4}$	[5 - 6]
$D_{GBM}\ [cm^2/h]$	$3.75\cdot10^{-6}$	[7]
$a\ [day^{-1}]$	$0.01 - 0.3$	[4]
$k\ [cells/cm^3]$	$\mathbf{10^6}$	[8]
Y	$10^6 - \mathbf{10^8}$	[9]
$\tau\ [h]$	$2 - 12$	[10]
$k_1\ [cm^3/h]$	$5\cdot10^{-10} - \mathbf{5\cdot10^{-8}}$	[9]
$k_2\ [h^{-1}]$	$1/(t^* - \tau)$	[9]
$k_3\ [h^{-1}]$	$0.014 - \mathbf{0.02} - 0.028$	[9]
$t^*[h]$	$36 - \mathbf{48} - 60$	[9]

Parameter sensitivity analysis

Parameters Y and k_1 have very wide ranges, spanning several orders of magnitude. Figure 3 shows how the front speed changes depending on these parameter values for model 2 and model 3.

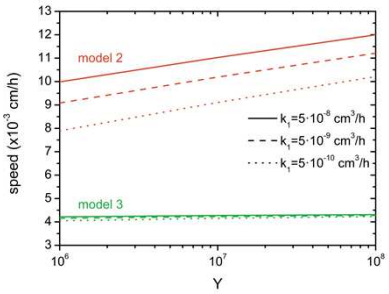

Fig. 3 VSV front speed on GBM for various values of Y and k_1. (Adapted from Fig. 4 in Ref. [3])

For our best framework, model 3, neither Y nor k_1 affect significantly the speed of the front.

For model 2, on the other hand, the results vary considerably with Y and k_1. Nonetheless, not even in the most favorable scenario, can it predict the observations.

Conclusions

We have described three increasingly realistic models to understand the dynamics of a virus-tumor system.

Our most complex model, which incorporates time-delay effects both in the reactive and diffusive terms, can satisfactorily predict the front speed for the lytic action of oncolytic VSV on GBM observed in vitro.

We have shown that the delay time τ is crucial in this reaction-diffusion models. For the VSV-GBM system our analysis predicts a range value of $5.0 < \tau < 9.3\ h$.

Our results for the in vitro front speed evidence that $c_{VSV} > c_{GBM}$, so theoretically the virus front could reach the tumoral front and cease its expansion.

[1] Wodarz, D. *et al.* PLoS Comp Biol. (2012) 8(6): e1002547
[2] Nowak, M. and May, RM. Virus dynamics. Mathematical principles of Immunology and Virology. Oxford (2000) pp. 100-109
[3] de Rioja, VL. *et al.* Biol. Direct (2016) 11: 1
[4] Stein, AM. *et al.* Biophys. J. (2007) 92(1): 356-365
[5] Ware, BR. *et al.* J. Virol. (1973) 11(1): 141-145
[6] Amor, DR. and Fort, J. Phys. Rev. E (2010) 82: 061905
[7] Fort, J. and Solé, RV. New J. Phys. (2013) 15: 055001-10
[8] Friedman, A. *et al.* Cancer Res. (2006) 66(4): 2314-19
[9] Wollmann, G. *et al.* J. Virol. (2010) 84(3): 1563-73
[10] Wollmann, G. *et al.* J. Virol. (2005) 79(10): 6005-22